37. BASEMENT ROCKS FROM THE EAST PACIFIC RISE NEAR 9°N COMPARED WITH OTHER OCEAN-FLOOR VOLCANIC PROVINCES

R. Hekinian and J. M. Morel,[1] Centre National pour l'Exploitation des Océans Centre Océanologique de Bretagne, Plouzane, France

INTRODUCTION

The East Pacific Rise (EPR) has an "S" shape extending from the Gulf of California to the southwestern Pacific Ocean where it joins the Mid-Indian Oceanic Ridge in the Tasman Sea region. The length of the EPR is about 17,000 km; its width is about 2000 km—comparable to that of the Mid-Atlantic Ridge (MAR). Previous petrological work on the EPR has been limited to dredged samples sporadically dispersed along the Rise (Engel and Engel, 1963, 1964; Chaynikov and Repecha, 1967; Bonatti, 1968; Hekinian, 1971; Batiza et al., 1977; Melson et al., 1977). (Figure 1). Compositional differences between EPR volcanic rocks and MAR rocks have been pointed out by previous authors. Scheidegger (1973), applying the plagioclase thermometry of plagioclase-bearing basalt, suggested that the fast-spreading EPR and slow-spreading MAR rocks have magma termperatures as well as plagioclase anorthite contents that are inversely correlated with the spreading rates. Investigation of the major-element chemistry of EPR samples has brought some students (Scheidegger, 1973; Clague and Bunch, 1976) to suggest that EPR volcanic rocks are derived by means of shallow crystal fractionation of more primitive magmas rather than by different depths of magma generation.

The area of the EPR explored by the D/V *Glomar Challenger* on Leg 54 is located between 8° and 9° North on the western flank of the Rise (Figure 1). The primary objective of this cruise, to drill a deep re-entry hole into a typical segment of fast-spreading oceanic crust, was not achieved because of inability to penetrate basaltic basement (Chapter 1, this volume). The shallow holes we did manage to drill fulfilled a secondary objective, to make a drilling transect perpendicular to the axis of the EPR in order to establish a temporal variation and a timing of eruptive events for a fast-spreading ridge. The age of the crust in the area of drilling ranges between 1.2 and 4.3 m.y. and was defined by using the marine magnetic anomalies recognized in the area. Details of the structural and geophysical aspects of this region have been described elsewhere (Rosendahl and Dorman, this volume).

Seven holes penetrating the basement to depths between 16 and 53 meters were drilled near 9°N on the EPR (Table 1). From these, four (Holes 429A, 420, 421, and 423) yielded samples of basement rocks associated with normal fabric structure; that is, features consisting of roughly north-south, small, elongated, abyssal hills (•100 m high) and troughs (Figure 1) that are believed to be morphological features associated with accreting plate boundary regions. Other holes (Holes 422, 428, and 428A) were drilled on flat-lying ponds of acoustically stratified sediment underlain by horizontal, strong reflectors at less than 6 km, respectively, north and south of the axis of an east-west linear volcanic structure called the OCP (Ocean Crust Panel) Ridge (Figure 2). Finally, Hole 427 was also drilled on a flat reflective basement located on the southern wall of the Siqueiros transform fault on crust that is about 1-2 m.y. old (Figure 2).

The present work comprises a preliminary study of basement rocks recovered from the EPR near 9°N and has as its main purpose the definition of the basaltic rock types encountered in relation to other volcanic rocks from various oceanic provinces. Bulk-rock compositional variations of the EPR are compared with some of the better known petrographic provinces of the MAR. In addition, the petrology of the Leg 54 basalts from 9°N is compared with that of other EPR samples located along the ridge system at various latitudes. Finally, some attempt is made to detect any compositional similarities between the volcanic rocks of the EPR and the rocks from aseismic ridges around the world.

PETROLOGY OF THE EPR ROCKS FROM NEAR 9°N

Minerals within the basaltic rocks from near 9°N on the EPR are essentially plagioclase and clinopyroxene. In the most crystalline specimens, the amount of clinopyroxene almost equals that of plagioclase (Table 2; Figure 3). The general texture of the rocks ranges from subophitic, through intersertal to hyalocrystalline. In most cases the two major mineral constituents, plagioclase and clinopyroxene, interlock and form equal-sized grains (<0.9 mm in diameter). In the least crystalline specimens, clusters of plagioclase and clinopyroxene abound while olivine is totally absent or present only in trace amounts. Olivine occurs in Sections 422-9-3, 428A-1-1, and 429A-2-1 (Table 2). The olivine of these rocks occurs as matrix constituents and rarely attains phenocryst size. A ternary diagram (Figure 4) shows the modal distribution of plagioclase, clinopyroxene, and olivine of Leg 54 basaltic rocks. Most of the samples fall near the cotectic line representing the liquid-crystal line of descent, as defined by Osborn and Tait (1952) for 1

[1] Present address: (J. M. Morel) Université de Bretagne Occidentale, Département de Géologie, Avenue le Gorgeu, Brest, France.

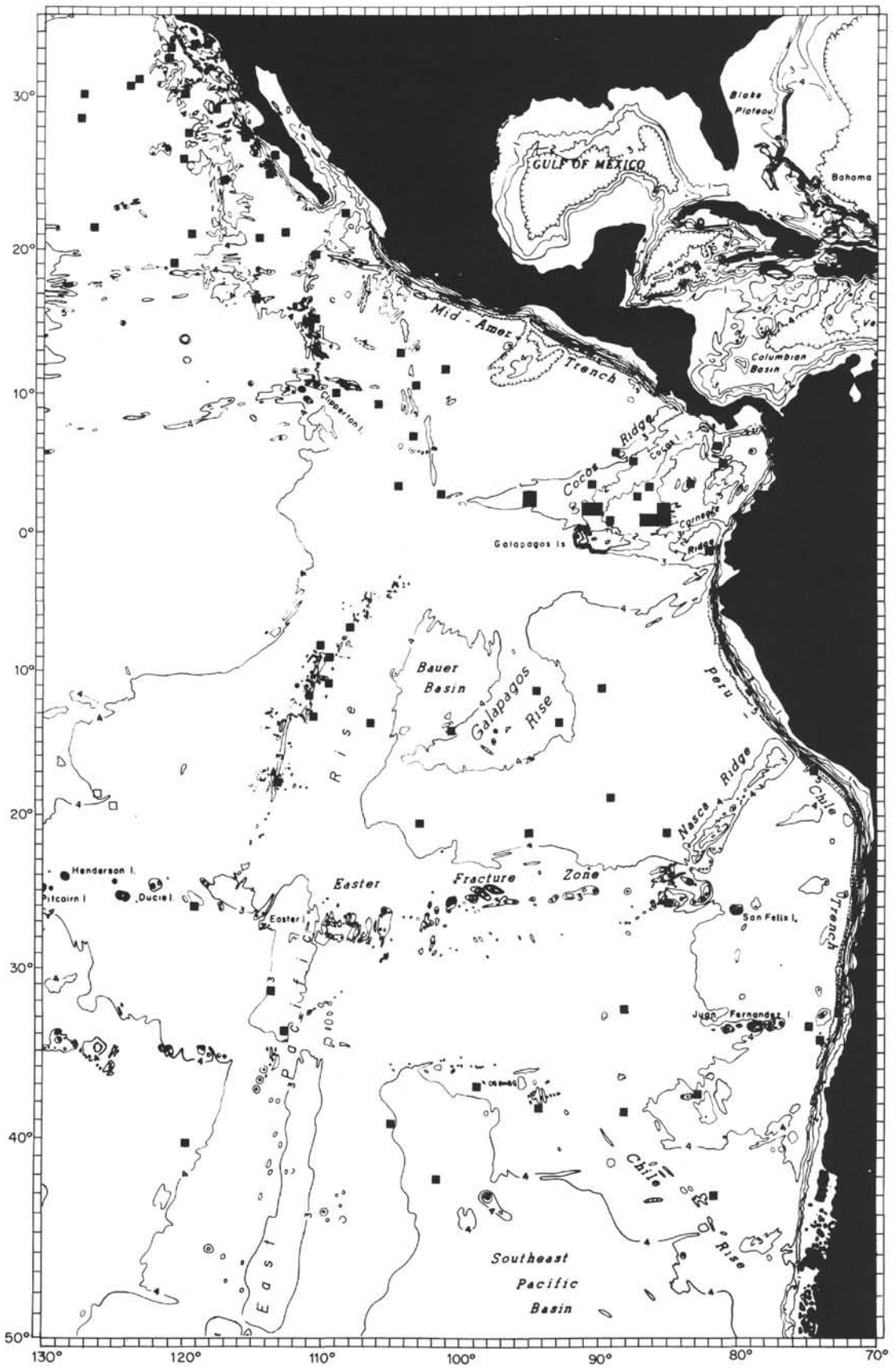

Figure 1. *Generalized bathymetric chart of the EPR after Chase (1975), showing the distribution of rock samples. The samples from the Galapagos region and those from the coastal area of Baja California are not included in this study.*

TABLE 1
Drilling Site Locations on the EPR near 9° N, Leg 54

Hole	Latitude	Longitude	Water Depth (m)	Basement Recovery
420	09°00.10'N	106°06.77'W	3381	1.22
421	09°01.41'N	106°03.68'W	3339	1.63
422	09°08.81'N	105°16.27'W	3247	9.56
423	09°08.81'N	105°06.57'W	3161	0.87
427	08°06.79'N	104°36.35'W	3834	12.51
428	09°02.77'N	105°26.14'W	3295	2.14
428A	09°02.77'N	105°26.14'W	3286	12.60
429A	09°02.01'N	106°45.87'W	3426	2.95

atm (Figure 4). Only a few samples of glassy rocks representing chilled margins are near the plagioclase corner and few contain early-formed plagioclase. Combining both mineralogical characteristics and chemical variations, we divided the rocks from 9°N into three distinct groups:

1) Plagioclase-pyroxene-olivine basalts (Holes 422, 428, 428A, 429, and 429A) containing mostly plagioclase, clinopyroxene, and olivine (1 to 9%), and having a TiO_2 content of about 1.4 per cent, a FeO* content of 7 to 11 per cent, and C. I. values higher than 50 (Tables 2 and 3; Figures 4 and 5).

2) Ferrobasalts (Holes 427 and 421) rich in plagioclase and clinopyroxene with a relatively high TiO_2 content (>2.3%), high FeO* (expressing total iron) content (>12 per cent) and a C. I. (Crystallization Index, of Poldervaart and Parker, 1964) of less than 41 (Tables 2, 4, and 5; Figures 4 and 5). The C. I. refers to the converted, normative minerals of the petrogeny's primitive system represented mainly by the anorthite, forsterite, and pyroxene contents (see Poldervaart and Parker, 1964, for details).

3) Plagioclase-pyroxene basalts (Holes 420, 421, 423, 429A, and 427) made up essentially of clinopyroxene and plagioclase with a TiO_2 content of less than 2.3 per cent, a FeO* content of less than 12 per cent, and a C. I. higher than 42 (Tables 2, 4, and 5; Figures 4 and 5).

From this classification it appears that a single hole into the basement may penetrate various types of basaltic rocks. Chemical analyses of the major and minor constituents are reported on a histogram in Figure 6. This shows that there is a compositional similarity among all the samples with respect to the SiO_2 (49 to 52%), K_2O (0.1 to 0.5%), and Na_2O (2 to 3%) contents (Figure 6), whereas bimodal and trimodal distributions are recognized for the other oxides such as CaO, MgO, Al_2O_3, TiO_2, and FeO contents (Figure 6). Thus the ferrobasalts from Hole 427 have higher FeO (12 to 14%) and TiO_2 (2.3 to 2.7%) contents than those of the other holes, except for some Hole 429A samples (Figure 6; Table 4). The olivine-bearing basalts of Holes 428, 428A and 422 have the lowest FeO* (7 to 10%) and TiO_2 (1 to 1.7%) contents (Figure 6). Intermediate values of these oxides are found among the plagioclase-pyroxene basalts from Holes 420, 421, and 423, and some from Hole 429A (Figure 6). Also the most aluminous type of basalts are found among the samples collected in Hole 422, where the Al_2O_3 content is about 15 to 17 per cent (Figure 6). Hole 427 contains the least aluminous basalts ($Al_2O_3 < 14\%$) (Figure 6).

Selected analyses of Leg 54 basaltic rocks are plotted on expanded ternary AFM diagrams (Figure 7). The corners of these diagrams represent the enlarged field at FeO* = 64, $Na_2O + K_2O$ = 38, and MgO = 50 (Figure 7). The basaltic rocks from the normal fabric of the EPR near 9°N are grouped into two distinct fields represented by Holes 422 and 428 closer to the MgO corner, while Holes 420, 421, 423, and 429A are all closer to the FeO* corner of the diagram (Figure 7). Apparently, there are no compositional differences between the normal fabric samples and those from the Siqueiros fracture zone (Figure 7). The latter samples are also divided into two main fields: those enriched in MgO, located mainly on an east-west transverse ridge as described by Batiza et al. (1977), and those depleted in MgO and high in FeO content such as the ferrobasalts from Holes 427 (Figure 7). These dredged samples from the transverse ridge regions show a variability trend (AFM diagram, Figure 7) comparable to that encountered in Holes 428, 428A, and 422 drilled at about 5 km from the axis of another east-west trending structure (OCP Ridge) located on the western flank at the EPR near 9°N (Figures 2 and 7). Both the OCP and the east-west trending ridge of the Siqueiros fracture zone are olivine-bearing basalts. The most differentiated rock in the mafic sense, formed on the east-west structural high off the Siqueiros fracture zone, is a picritic basalt containing up to about 30 per cent of olivine phenocrysts (Batiza et al., 1977; Schrader et al., this volume).

Both mineralogical and chemical variations thus indicate that there are no major differences among the volcanic rocks found associated with the various tectonic provinces such as the "normal fabric area" along the EPR flank regions and the samples (Hole 427) from the Siqueiros fracture zone (Figure 2, 3, and 4). In addition, there is no evidence of compositional changes of the volcanic products forming the crust along a westward transect perpendicular to the EPR axis.

COMPARISON OF LEG 54 ROCKS WITH OTHER VOLCANIC PROVINCES

When comparing volcanic rocks from various oceanic provinces, we have to consider the scarcity of data and the geographic extent of the regions involved. The difficulties encountered are mainly related to the number of samples studied from each region and how representative they are of a particular area. However, with the data at hand, a comparison of compositional variations over different regions of the ocean floor might throw some light on the relationship between composition and structural setting.

EPR

Among the regions sampled along this Rise between 45°N and 56°S, which are about 9000 km apart, there are only five areas that have sufficient data to use for a regional comparative study; these are located near 44°N

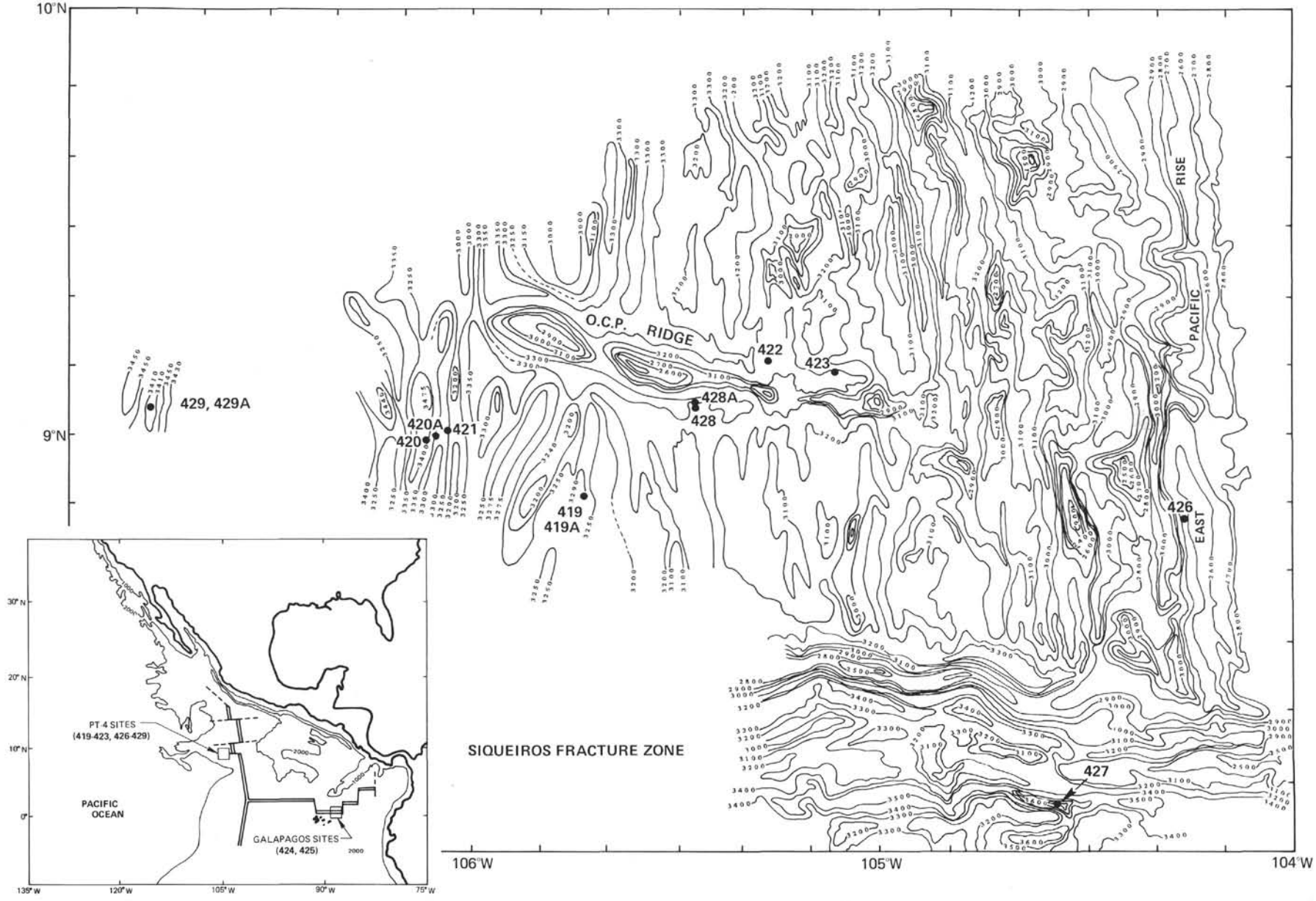

Figure 2. *Bathymetric map of the EPR near 9°N, showing the locations of drilled holes on Leg 54.*

TABLE 2
Modal Analysis Results (vol. %) of Basaltic Rocks Collected on Leg 54 from the East Pacific Rise near 9° N[a]

Mineral \ Sample (Interval in cm)	420-13, CC, 50–57	420-14-1, 1–8	420-15-1, 2-22 Average of four	421-3-1, 28–148 Average of three	422-7-1, 20–131 Average of three	422-9-3, 80–95	422-9-4, 94–97	423-8-1, 50–52	428-6-1, 74–79	428A-1-1, 92–94	428A-4-1, 50–117 Average of two	428A-4-1, 15–96 Average of two	429-2-1, 87–89	427-9-4, 427-10-4 Average of two	427-9-1, 0–7
Plagioclase	18.4	46.5	12.5	47.0	41.8	52.6	44.4	10.0	48.0	50.3	50.2	49.8	35.3	55.4	16.1
Pyroxene	4.7	27.7	3.6	32.5	46.4	34.2	42.4	14.2	28.1	27.3	28.3	28.4	43.7	32.1	9.8
Olivine	–	–	0.9	–	tr.	9.4	4.9	1.6	0.4	1.5	–	2.5	6.7	–	–
Phyllosilicates	2.1	0.2	tr.	1.73	–	–	–	–	–	–	–	–	–	2.1	–
Mesostasis	70.8	24.1	81.8	12.4	11.3	3.5	10.0	72.5	22.0	20.2	21.3	19.4	13.4	4.8	72.2
Vesicles	3.3	1.5	1.3	–	<1	1.3	–	–	–	–	–	–	–	0.2	2.3

[a]Data obtained onboard *Glomar Challenger* and included in Site Report.
Note: The Mesostasis includes glass cryptocrystalline material and iron oxide minerals. Calcite and zeolite were found in trace amount. Hole 427 is on the Siqueiros transform fault.

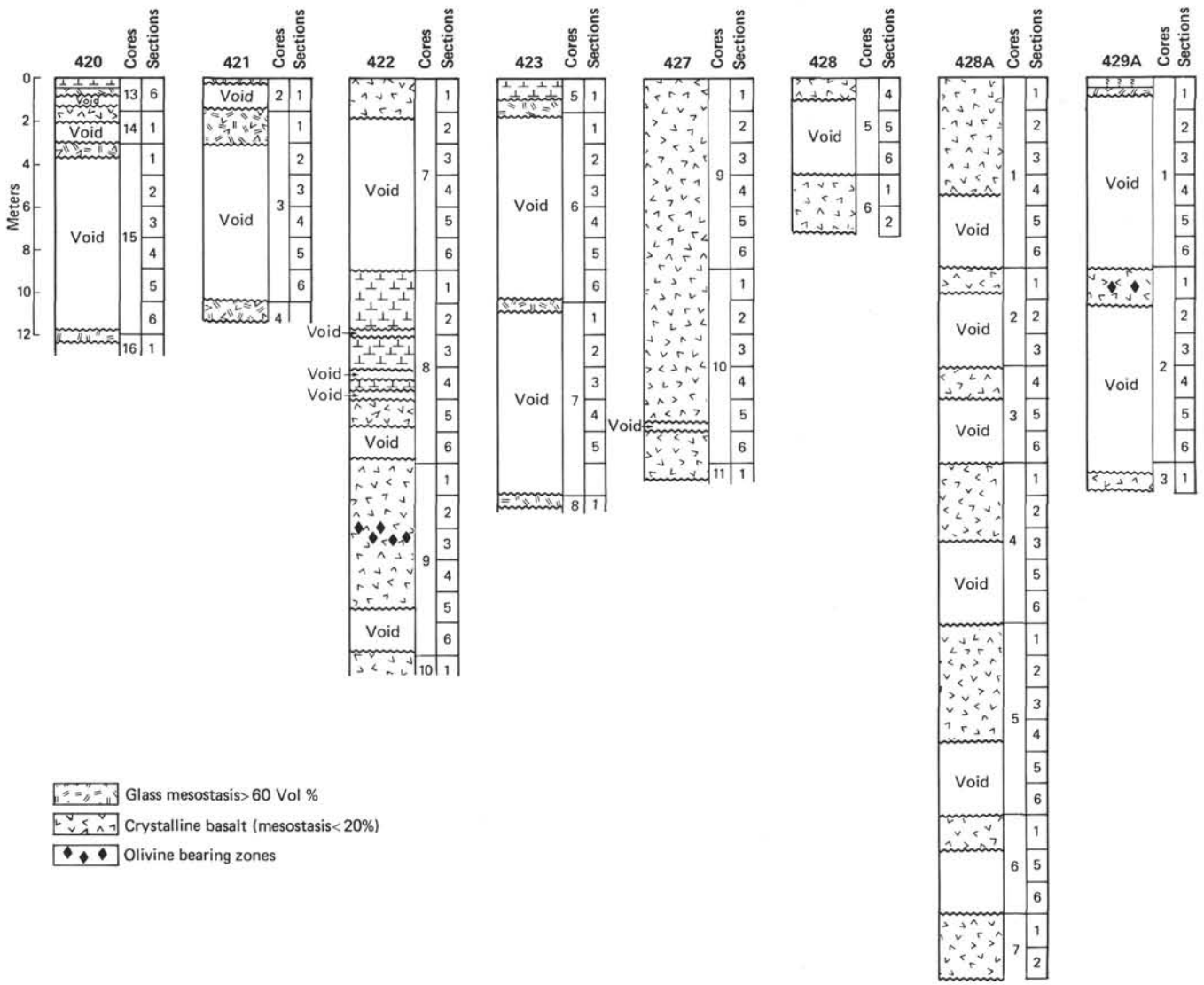

Figure 3. *Lithological columns of basement rocks drilled during Leg 54 in the EPR near 9°N.*

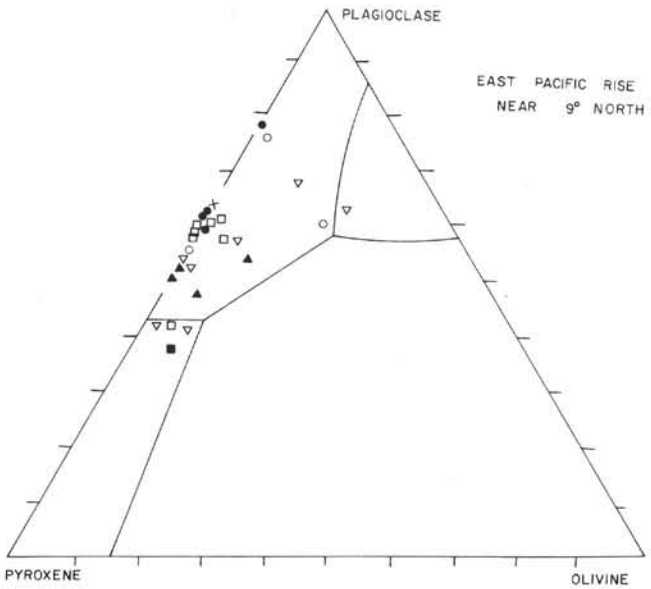

Figure 4. *Ternary diagram for modal olivine, plagioclase, and clinopyroxene content of Leg 54 rocks collected from the EPR 9°N (○) indicates samples from Hole 421. (●) indicates Hole 420. (▲) stands for Hole 422, and (■) indicates Hole 423. (×) is a sample from Hole 427. (□) indicates Hole 428A, and (▽) stands for Hole 429A. The continuous lines define the fields specified by the experimentally derived (at 1 atm) reaction lines of Osborn and Tait (1952).*

(Juan De Fuca), 42°N (Gorda Rise), 21°N, 9°N (Siqueiros region), and 13°S. Within these areas, the surface coverage of dredge and drill sites is highly variable. For example, near 21°N the sampling area is less than 50 km². At 9°N, fewer than 20 dredges and seven drill holes obtaining basement rocks were in a corridor of about 130 km long and 20 km wide.

In order to extend the collection of data, for our purposes we have used all samples located on crust less than 10 m.y. old. The geographical extent along the EPR of this age boundary was taken from the magnetic anomaly map of Pitman et al. (1975).

Compositions obtained by microprobe analyses on basalt glassy margins of samples recovered from the various segments of the EPR are plotted on Figure 8. This shows the TiO_2 contents and FeO* (total Fe calculated as FeO)/MgO ratio of glassy basalts versus the half-spreading rate calculated (after Minster et al., 1977) for each sample location on the various segments of the Rise (Morel, in press). Because microprobe analyses of glassy margins from Leg 54 drilled basalts were not available at the time of this writing, bulk-rock analyses of aphyric samples (i.e., most of the basalts) were used. Glass analyses since obtained on Leg 54 basalts (Natland and Melson, this volume) conform closely to aphyric basalt whole-rock compositions.

When the overall data, comprising the most heavily sampled regions, are considered together with the scattered rocks sampled along the other segments of the

TABLE 3
Chemical Analysis Results (wt. %) of Olivine-Bearing Basalts Collected on Leg 54 at the EPR near 9° N[a]

Sample (Interval in cm)	422-10-1, 19-25	422-7-1, 20-25	422-7-2 (Piece 3)	422-8-5, 132-135	422-9-1, 70-73	422-9-3, 91-94	422-9-5, 72-75	428-6-2, 1-3	428A-1-1, 21-23	428A-1-1, 27-29	428A-1-2, 49-51
SiO_2	50.39	50.49	50.74	50.73	50.28	48.59	49.77	50.01	50.87	50.48	50.45
Al_2O_3	13.92	14.17	14.28	14.32	13.99	15.50	15.83	14.17	14.61	14.53	14.28
Fe_2O_3	3.04	3.26	2.15	2.40	2.26	2.31	2.37	3.19	2.99	3.28	3.48
FeO	7.92	6.61	7.59	7.25	7.55	6.36	6.68	6.54	6.72	6.16	6.58
MnO	0.20	0.17	0.18	0.17	0.17	0.19	0.15	0.20	0.31	0.32	0.19
MgO	7.09	7.83	8.04	8.21	7.87	8.45	8.63	7.52	7.31	7.05	7.40
CaO	11.72	11.98	12.00	11.99	11.92	11.59	11.68	11.84	11.87	12.26	12.03
Na_2O	2.94	2.39	2.70	2.74	2.71	2.85	2.83	2.44	2.50	2.60	2.50
K_2O	0.31	0.13	0.13	0.10	0.09	0.23	0.21	0.08	0.23	0.10	0.17
TiO_2	1.88	1.44	1.45	1.45	1.43	1.38	1.43	1.45	1.48	1.48	1.50
P_2O_5	0.21	0.17	0.15	0.17	0.15	0.18	0.18	0.14	0.16	0.14	0.16
CO_2	0.00	0.00	0.00	0.00	0.00	0.00	0.00	0.00	0.00	0.00	0.00
L.O.I.	0.00	0.76	0.21	0.14	1.04	1.33	0.33	0.36	0.00	0.50	0.33
TOTAL	99.61	99.39	99.61	99.66	99.45	98.95	100.08	97.93	99.04	98.89	99.06
Q	0.00	2.51	0.00	0.00	0.00	0.00	0.00	2.53	2.37	2.47	2.45
or	1.83	0.76	0.76	0.59	0.53	1.35	1.24	0.47	1.35	0.59	1.00
ab	24.87	20.22	22.84	23.18	22.93	24.11	23.94	20.64	21.15	22.00	21.15
an	23.87	27.55	26.46	26.47	25.74	28.82	29.87	27.47	27.96	27.68	27.24
di	26.67	24.73	25.98	25.75	26.25	22.09	21.62	24.41	24.10	25.91	25.24
hy	13.59	15.00	16.05	15.94	16.07	6.04	9.24	14.33	14.57	11.85	13.38
ol	0.30	0.00	1.07	0.95	0.55	8.81	7.26	0.00	0.00	0.00	0.00
mt	4.40	4.72	3.11	3.47	3.27	3.34	3.43	4.62	4.33	4.75	5.04
ilm	3.57	2.73	2.75	2.75	2.71	2.62	2.71	2.75	2.81	2.81	2.84
ap	0.49	0.40	0.35	0.40	0.35	0.42	0.42	0.33	0.37	0.33	0.37
C.I.[b]	43.24	47.24	46.27	46.69	45.36	52.18	51.86	46.70	46.41	47.94	47.12

[a]Data from Joron, this volume.
[b]Indicates the Crystallization Index of Poldervaart and Parker, 1964.

TABLE 4
Chemical Analysis Results (wt. %) of Plagioclase-Pyroxene Basalts Collected on DSDP Leg 54 at the EPR near 9°N[a]

Sample (Interval in cm)	420-14-1, 0-8	420-17-1, 27-30	421-2-1, 5-7[b]	421-3-1, 117-120	421-4-1, 4-7	421 Bit 10-13	423-5, CC (40-42)	423-6-1, 28-34	423-8-1, 40-42	429A-1-1, 43-45	429A-3-1 (Piece 7)
SiO_2	50.43	50.67	50.32	51.54	51.49	50.24	50.43	50.14	50.90	49.72	50.57
Al_2O_3	13.77	14.28	13.11	14.14	14.04	13.85	13.59	13.40	13.55	15.87	13.89
Fe_2O_3	2.99	4.55	5.69	4.01	2.97	5.50	4.27	4.56	4.89	3.64	3.84
FeO	8.47	5.80	7.39	6.13	6.62	6.23	6.38	7.61	6.68	4.63	7.26
MnO	0.20	0.19	0.22	0.20	0.23	0.20	0.21	0.20	0.18	0.15	0.16
MgO	7.18	6.30	6.42	6.44	6.74	7.11	6.79	6.92	6.82	7.12	7.07
CaO	11.21	11.20	9.86	11.04	11.14	10.76	11.02	10.97	10.87	12.99	11.44
Na_2O	2.55	2.80	2.69	2.78	2.89	2.59	2.92	1.94	2.57	2.33	2.42
K_2O	0.16	0.43	0.44	0.37	0.37	0.45	0.32	0.23	0.35	0.08	0.08
TiO_2	1.94	1.99	2.54	2.15	2.22	2.12	2.09	2.06	2.10	1.15	1.61
P_2O_5	0.19	0.16	0.23	0.19	0.22	0.19	0.24	0.23	0.22	0.11	1.15
CO_2	0.00	0.00	0.00	0.00	0.00	0.00	0.00	0.00	0.00	0.00	0.00
L.O.I.	0.14	1.10	0.83	0.86	0.67	0.76	1.14	0.83	0.81	0.98	0.43
TOTAL	99.22	99.46	99.73	99.84	99.59	99.99	99.39	99.08	99.93	98.76	99.91
Q	2.33	4.34	6.02	5.22	3.41	4.51	3.32	7.09	5.52	2.67	5.67
or	0.94	2.54	2.60	2.18	2.18	2.65	1.89	1.35	2.06	0.47	0.47
ab	21.57	23.69	22.76	23.52	24.45	21.91	24.70	16.41	21.74	19.71	20.47
an	25.65	25.12	22.39	25.01	24.24	24.83	23.02	27.17	24.40	32.60	26.80
di	23.34	23.41	20.02	22.79	23.78	21.68	24.04	20.74	22.45	24.72	18.10
hy	16.78	8.50	11.49	9.91	11.81	11.19	10.54	14.42	11.35	9.87	16.66
mt	4.33	6.59	8.24	5.81	4.30	7.97	6.19	6.61	7.09	5.27	5.56
ilm	3.68	3.77	4.82	4.08	4.21	4.02	3.96	3.91	3.98	2.18	3.05
ap	0.44	0.37	0.54	0.44	0.51	0.44	0.56	0.54	0.51	0.25	2.71
C.I.[c]	42.29	45.00	38.95	43.88	42.91	44.05	42.86	43.41	43.08	54.19	41.02

[a]Data from Joron et al., this volume.
[b]This sample is a ferrobasalt.
[c]Indicates the Crystallization Index of Poldervaart and Parker, 1964.

EPR, no prominent crustal compositional variations are found to correlate with the spreading rate (Figure 8). This may be because there is not enough sample coverage on rise segments with fast spreading rate (7–9 cm/y., half-spreading rate; Figure 8). Also, tectonically the Juan de Fuca and Gorda Rises might represent anomalous ridge systems, since they are separated from the bulk of the EPR by several thousand kilometers along a complex transform fault system which crosses a portion of the North American continent. Their physiography is similar to that of portions of the Galapagos Spreading Center. When considering only the most heavily sampled areas (45°N, 42°N, 21°N, 9°N, and 13°S), however, a positive correlation between the basalt compositional range and the rate of spreading does exist (Figure 8). The basalts erupted at slow spreading ridges (<2 cm/y., half rate) have low TiO_2 contents (<1.6%) and low FeO*/MgO ratios (<1.7). Intermediate (3-6 cm/y. half rates) and fast spreading systems erupt basalts with TiO_2 contents of 1.3 to 2.5 per cent, and greater than 2 per cent, respectively (Figure 8).

A sharp compositional contrast exists between the glassy basalt samples analyzed from the northern Mid-Atlantic Ridge (<2 cm/y. half rate) and those found on the various segments of the EPR having intermediate to fast spreading rates (Figure 8). Most of the MAR glassy basalts have lower TiO_2 contents (<1.4%) and FeO*/MgO ratios (<1.8) than those of the EPR samples.

MAR Compared With Pacific-Ocean-Floor Volcanic Rocks

Chemical variation expressed in terms of the FeO*/MgO ratio of basaltic rocks collected along the MAR within a crust that is less than 10 m.y. old is shown in Figure 9. The range of FeO*/MgO variability (0.4 to 3) for the rocks located between about 77°N and about 22°N latitude is constant (Figure 9). However, chemical analyses of the basaltic chilled margin collected from various segments of the MAR show a compositional difference between volcanics erupted north of latitude 33°N and those south of it (Morel and Hekinian, in preparation).

In order to compare volcanic rocks from major oceanic ridge systems such as the MAR and the EPR, two types of ternary diagrams are used:

1) An AFM diagram (alkali, iron oxide, and magnesia) showing the plots of MAR volcanic rocks at 45°N (Aumento, 1968; Muir et al., 1964), at near 36°50′N (Arcyana, 1977; Hekinian et al., 1976; Aumento, Melson, et al., 1977) and from 22°N (data from Legs 45 and 46; Bougault et al., 1978). In addition, plots of various Eastern Pacific provinces such as basin areas (Yeats et al., 1973) and seamount provinces (Engel and Engel, 1964) are shown (Figure 10).

TABLE 5
Chemical Analysis Results (wt. %) of Ferrobasalts Collected From the Siqueiros Fracture Zone at the EPR near 8° N, on Leg 54[a]

Sample (Interval in cm)	427-9-3, 16-19	427-10-1, 64-67	427-10-5, 82-84
SiO_2	49.78	49.41	49.88
Al_2O_3	13.05	13.25	13.26
Fe_2O_3	5.10	5.18	4.85
FeO	8.21	7.89	8.00
MnO	0.20	0.22	0.19
MgO	6.59	6.78	6.80
CaO	10.15	10.21	10.31
Na_2O	2.83	2.11	3.02
K_2O	0.07	0.08	0.06
TiO_2	2.48	2.46	2.41
P_2O_5	0.25	0.26	0.27
CO_2	0.00	0.00	0.00
L.O.I.	0.29	0.67	0.10
TOTAL	98.99	98.51	99.14
Q	4.55	7.45	3.22
or	0.41	0.47	0.35
ab	23.94	17.85	25.55
an	22.69	26.44	22.44
di	20.98	18.10	21.70
hy	13.42	14.73	13.53
mt	7.39	7.51	7.03
ilm	4.71	4.67	4.57
ap	0.58	0.61	0.63
C.I.	38.85	41.03	39.32

[a]Data from Joron et al., this volume.

2) An AFT (Alumina-ferromagnesia-titania: Al_2O_3 + CaO/SiO_2-MgO/FeO-TiO_2) diagram shows the same rock distribution as the AFM diagram (Figures 10 and 11) but has the advantage of emphasizing the contribution of plagioclase in differentiating the various types of basaltic rocks. The oxide content in weight per cent forming the apex of the diagram of Figure 11 is influenced by the relative proportion of the plagioclase and the ferromagnesian minerals forming the rocks. The distribution pattern for the samples from the MAR shows two trends: one, an enrichment of the MgO/FeO ratio due to olivine accumulation, and the other a plagioclase increase toward the Al_2O_3 + CaO/SiO_2 corner (Figure 11). The samples plotting nearer the TiO_2 corner are characterized by rocks that are relatively rich in clinopyroxene and in cryptocrystalline matrix material (Figure 11). The basaltic rocks from the EPR, the Chile Rise, and the Pacific basin provinces (Nazca plate and northeast Pacific basin), with the exception of seamounts, show a linear trend going toward the TiO_2 corner, as plotted in Figure 11. This diagram does not show any trend deviating toward either the MgO/FeO or the Al_2O_3 + CaO/SiO_2 corner. This is consistent with the fact that abnormal accumulation of neither plagioclase nor olivine has been observed among the Eastern Pacific samples (i.e., the rocks are aphyric or only very sparsely phyric).

Recent Spreading Ridges Compared With Aseismic Ridges

Another type of oceanic province is the aseismic ridges which are considered to be chains of elevated volcanoes formed during the early history of ocean-floor crustal formation. Because aseismic ridges are older structures than recent spreading provinces, they are more inclined to have altered rock outcrops. To minimize the effects of alteration, some metals such as Ti and Zr—which are, to a certain extent, more resistant to weathering than other major elements—are plotted. Figure 12 shows the Ti and Zr variation diagram for rocks from the MAR and the average values of these elements for Leg 54 samples.

In addition, rocks from the Cocos, the Carnegie, the Walvis, and the Ninety East Ridges are shown in the same diagram (Figure 12). Low Ti (<1000 ppm) and low Zr (<140 ppm) content are represented by volcanic rocks from the MAR (FAMOUS area and 45°N) (Figure 12), whereas higher values of Ti (1000 to 1500 ppm) are found in samples from the EPR areas near 9°N (Leg 54). The Leg 54 samples are similar, with respect to their Ti and Zr contents, to those obtained from aseismic ridges (Figure 12). For instance, the ferrobasalts from the Ninety East Ridge in the Indian Ocean and the basalts from the Carnegie and Cocos Ridges have comparable Ti (1000 to 2000 ppm) and Zr (100 to 300 ppm) contents (Figure 12). The increase in Ti and Zr contents seems to be accompanied by an enrichment in clinopyroxene when compared to the average ocean-floor basalt from the MAR.

CONCLUSIONS

The basaltic rocks collected on Leg 54 near 9°N on the EPR are divided into three categories:

1) Ferrobasalts (TiO_2 >2-3%; FeO >12%) found mostly at Hole 427 of the Siqueiros transform fault;

2) Plagioclase-pyroxene basalts (TiO_2 <2-3% and FeO <12%) found at Sites 420, 421, 423, and 429, located on the EPR normal fabric type of structure, and

3) A plagioclase-pyroxene-olivine basalt (TiO_2 ≅1.4%, FeO = 7-11%) found mainly at Sites 422 and 428 located on a small ponded type of structure in the vicinities of the east-west trending OCP Ridge.

Both bulk-rock and glassy basalt analyses indicate that a sharp compositional difference exists between the volcanic rocks erupted on various structures of the EPR near 9°N on the one hand and those of the northern part of the Mid-Atlantic Ridge, on the other hand.

When considering the most heavily sampled regions along various segments of the EPR and the Northern Atlantic Ridge, a positive correlation is observed between the compositional variation of glassy basalt margins (and aphyric rocks) and the rate of spreading. Volcanic rocks erupted on oceanic ridge segments with slow spreading rates (<2 cm/y., half rate) contain a low FeO*/MgO (<1.7 and low TiO_2 content (<1.6%). Ridge segments with intermediate rates of spreading (3-6 cm/y.) consist of a lava with a FeO*/MgO ratio of

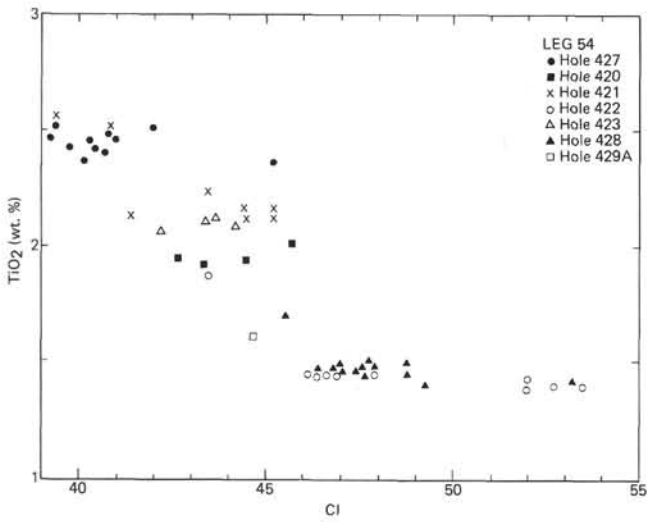

Figure 5. *TiO_2 and C.I. (Crystallization Index of Poldervaart and Parker, 1964) of rocks from Leg 54 holes on the EPR near 9°N. The samples with C.I. higher than 50 contain a fair amount of olivine.*

1.2–2.1 and a TiO_2 content of 1.3–2.5%. Fast spreading ridges (>6 cm/y., half rate) are characterized by eruptive flows with the highest TiO_2 content (>2%) and the highest FeO*/MgO ratios (>1.8). Further sampling sites, mainly on fast spreading segments of the EPR, are needed to corroborate the forementioned relationship.

Available data on the Zr and Ti content of volcanic rocks from different structural settings seem to indicate that Leg 54 samples have compositions similar to basaltic rocks found on some aseismic ridges, such as the Ninety East Ridge (Indian Ocean) and the Cocos and Carnegie Ridges (eastern Pacific Ocean).

ACKNOWLEDGMENTS

We are grateful to the Captain, the ship's crew, the drilling crew, and the laboratory technicians of the *Glomar Challenger* for the considerable assistance rendered in obtaining and handling the samples on Leg 54. We also thank the DSDP organizer for having invited one of us to participate in this cruise. The XRF analyses were done onshore by L. Briqueu. The FeO contents were determined at the C. R. P. G. in Nancy (France).

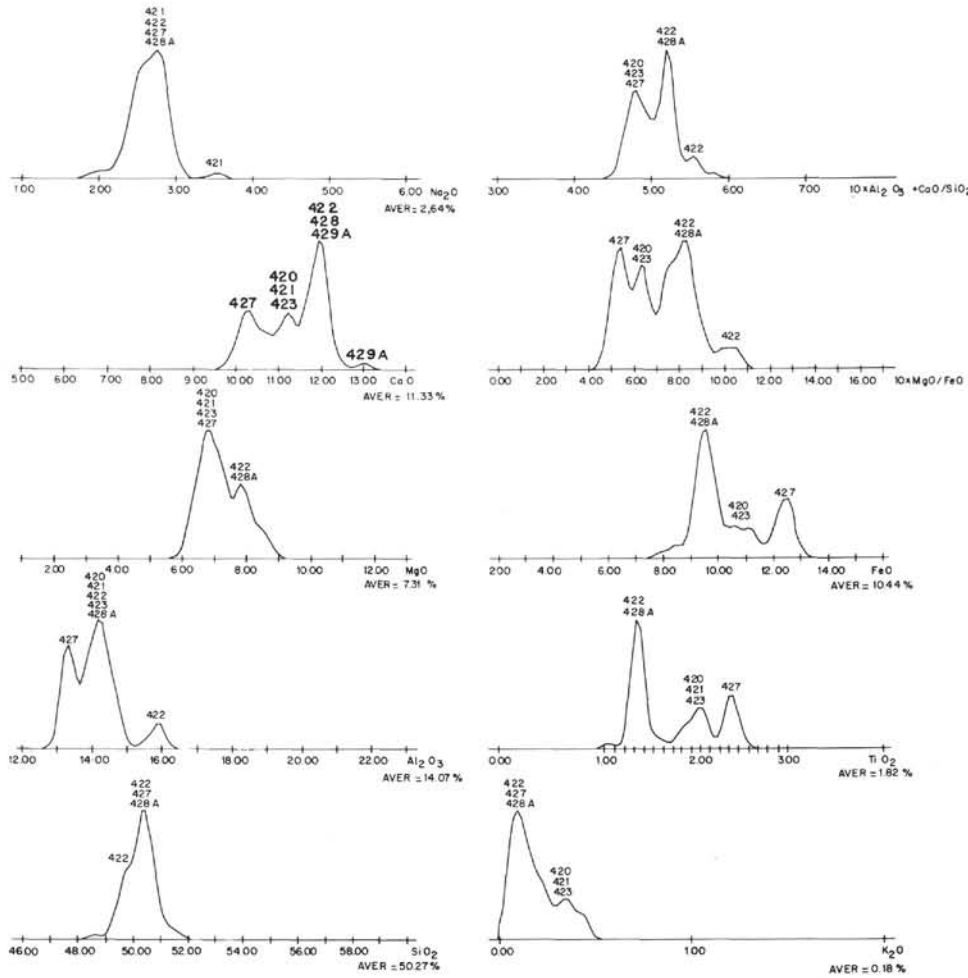

Figure 6. *Histogram of 66 analyses of basaltic rock from Leg 54 from near 9°N on the EPR. The hole numbers are shown above the peaks of the graphs which represent the oxide contents in wt. %.*

REFERENCES

Arcyana, 1977. Rocks collected by bathyscaph and diving saucer in the FAMOUS area of the Mid-Atlantic Rift Valley: petrological diversity and structural setting. *Deep-Sea Res.*, v. 24, p. 565–589.

Aumento, F., 1968. The Mid-Atlantic Ridge near 45°N basalts from the area of Confederation Peak. *Can. J. Earth Sci.*, v. 5, p. 1–21.

Aumento, F., Melson, W. G., et al., 1977. *Initial Reports of the Deep Sea Drilling Project,* v. 37: Washington (U. S. Government Printing Office).

Batiza, R., Rosendahl, B. R., and Fisher, R. L., 1977. Evolution of the oceanic crust: petrology and chemistry of basalts from the East Pacific Rise and the Siqueiros transform fault. *J. Geophys. Res.* v. 82 (2), p. 265–276.

Bonatti, E., 1968. Fissure basalts and ocean floor spreading on the East Pacific Rise. *Science,* v. 161, p. 886–888.

Bougault, H., Treuil, M., and Joron, J. L., 1978. Trace elements from 23°N and 36°N in the Atlantic Ocean: fractional crystallization, partial melting and heterogeneity of the upper mantle material. *In* Melson, W. G., Rabinowitz, P. D., et al., *Initial Reports of the Deep Sea Drilling Project,* v. 45: Washington (U.S. Government Printing Office), p. 493–506.

Bunch, T. E. and Laborde, R., 1976. Mineralogy and composition of selected basalts from DSDP Leg 34. *In* Yeats, R. S., Hart, S. R., et al., *Initial Reports of the Deep Sea Drilling Project,* v. 34: Washington (U.S. Government Printing Office), p. 263–276.

Cann, J. R., 1969. Spilites from the Carlsberg Ridge, *Indian Ocean J. Petrol.*, v. 10 (1), p. 1–19.

———, 1970. Rb, Sr, Cr, Zr, and Nb in some ocean floor basaltic rocks. *Earth Planet. Sci. Letters,* v. 10, p. 7–11.

Chase, T. E., 1975. Topography of the oceans. IMR Technical Report Series, TR 57, Scripps Institution of Oceanography, University of California.

Chaynikov, V. I. and Repecha, M. A., 1967. A manifestation of submarine volcanism in the northeastern Pacific. *Dokl. Earth Sci. Sect.* v. 173, p. 239–240.

Clague, A. D. and Bunch, T. E., 1976. Formation of ferrobasalt at East Pacific Mid Ocean spreading centers. *J. Geophys. Res.*, v. 81 (23), p. 4247–4256.

Clark, J. G. and Dymond, J., 1977. Geochronology and petrochemistry of Eastern and Sala y Gomez islands: Implications for the origin of the Sala y Gomez ridge. *J. Volcanol. Geotherm. Res.*, v. 2, p. 29.

Corliss, J. B., Dymond, J., and Lopez, C., 1976. Elemental abundance patterns in Leg 34 rocks. *In* Yeats, R. S., Hart, S. R., et al., *Initial Reports of the Deep Sea Drilling Project,* v. 34: Washington (U.S. Government Printing Office), p. 293–299.

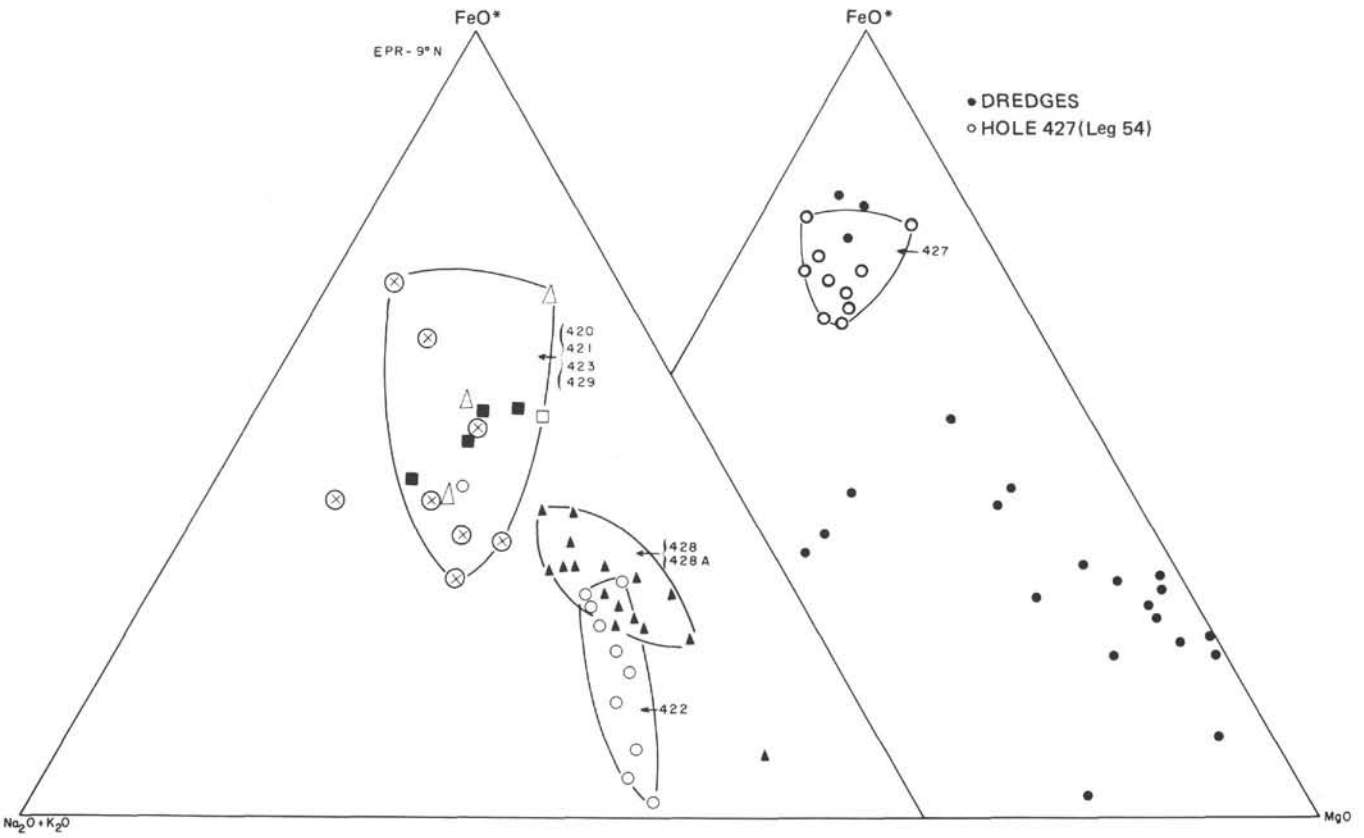

Figure 7. *AFM enlarged ternary diagram for the basaltic rocks from Leg 54. The corners of the triangles represent FeO* = 64; $Na_2O + K_2O$ = 38; and MgO = 50. The ternary diagram on the left represents the samples collected from the normal fabric of the EPR near 9°N; the diagram on the right represents the samples from the Siqueiros transform fault. The dredged samples are from Batiza et al. (1977). The symbols are as follows: (■) represents Hole 420, (×) indicates Hole 421, (○) stands for Hole 422, (Δ) indicates Hole 423, (▲) indicates Hole 428, and (■) stands for Hole 429A.*

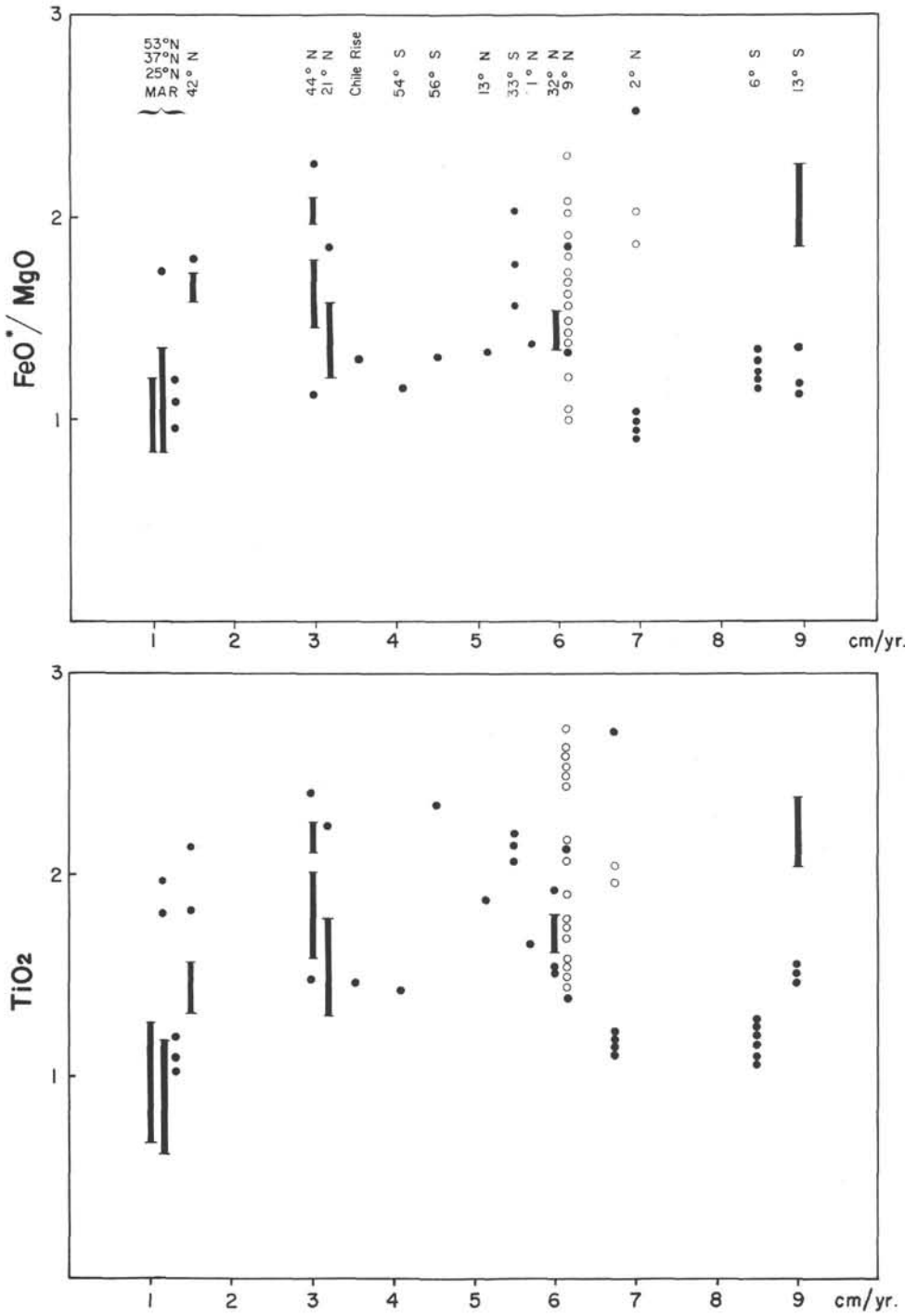

Figure 8. *FeO*/MgO and TiO_2 content of glassy basalt margins versus the half-spreading rate of various mid-oceanic ridge segments from the Atlantic (MAR) and Pacific oceans. The spreading at the sample locations was calculated using models from Minster et al. (1974). The sample designations and details of the spreading rates at various latitudes are given elsewhere (Morel, in press). Empty circles indicated the bulk-rock analyses of aphyric basalts from Leg 54. The two glassy basalt samples are from Humphris and Thompson (Site 420 and 429). The other two aphyric basalts from 2°N (empty circles) are from Leg 9 (Site 82). The approximate latitude of the sample locations is indicated on top of the diagram. The data on the glass are from Melson et al. (1977) and this work. The heavy lines indicate a concentration of data representing more than five samples.*

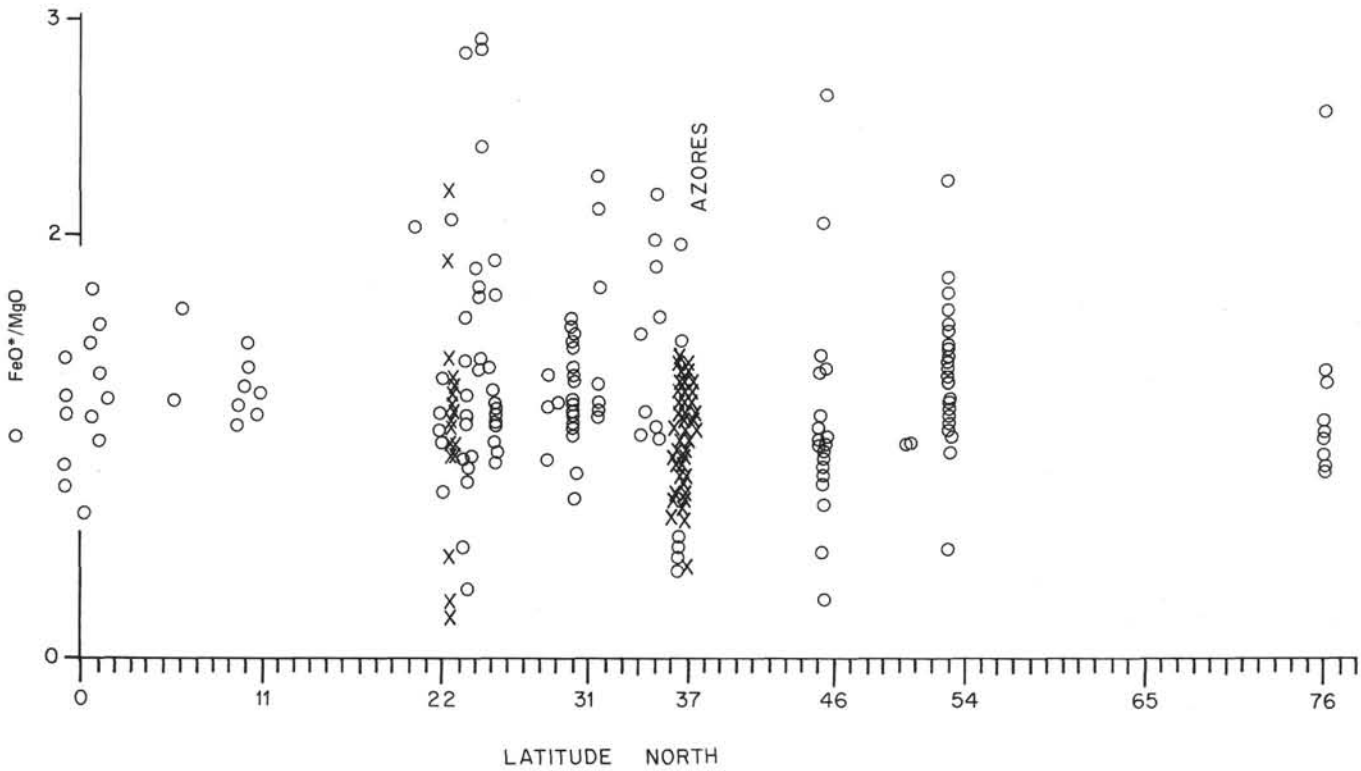

Figure 9. *FeO* (total iron as FeO)/MgO variation diagram for rocks collected at various latitudes along the MAR with crustal age of less than 10 m.y. The data source is from Aumento (1968); Miyashiro et al (1969); Engel and Engel (1964); Shido et al. (1971); Hekinian and Aumento (1973); Aumento, Melson et al. (1977); Melson et al. (1977); Arcyana (1977); and Bougault et al. (1978). (×) indicates glassy basalt data (present work) and (○) indicates bulk-rock analyses taken from the literature.*

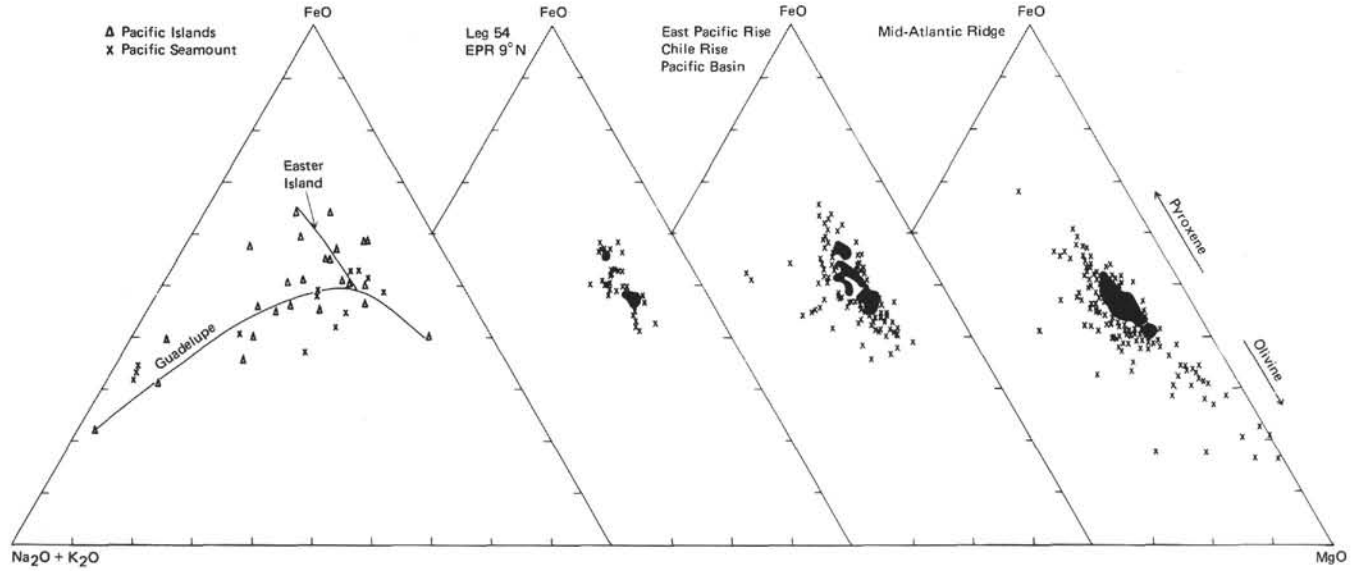

Figure 10. *AFM ternary diagram for rocks collected from various oceanic provinces of the Pacific and Atlantic oceans. The data sources from the Pacific seamounts and from the islands are from Engel and Engel (1961, 1963), Poldervaart and Green (1965), and Kay et al. (1970). The data on the Pacific Ocean rocks were from Luyendyk and Engel (1969), Hekinian (1971), Yeats et al. (1973), Kempe (1976), Thompson et al. (1976), Donaldson et al. (1976), Rhodes et al. (1976), Mazzullo et al. (1976), Bunch and Laborde (1976), Ridley and Ajdukiewicz (1976), Hart (1976), and Corliss et al. (1976). The rock samples from the Atlantic Ocean were taken from Muir et al. (1964), Aumento (1968), Miyashiro et al. (1969), Shido et al. (1971), and Hekinian and Aumento (1973).*

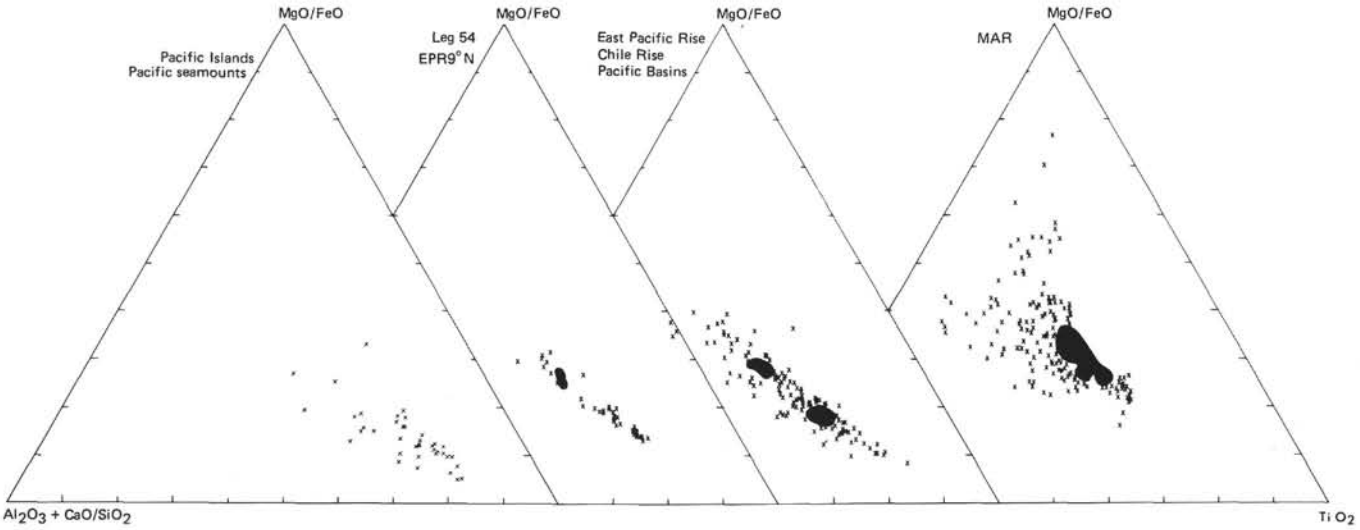

Figure 11. *AFT (alumina–ferromagnesia–titania) (Al_2O_3 + CaO/SIO_2 • 0.25–MgO/FeO–TiO_2) ternary diagram for rocks from various oceanic provinces of the Pacific and Atlantic oceans. The data sources are the same as in Figure 10.*

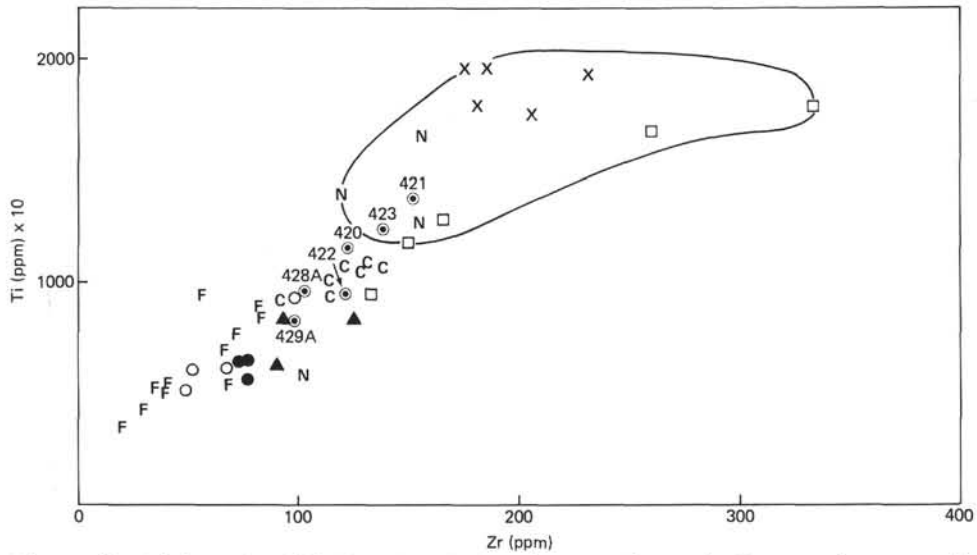

Figure 12. *Ti (ppm) and Zr (ppm) variation diagram for rocks from various oceanic provinces around the world. The average values for Leg 54 rocks are shown with their corresponding hole numbers. (F) indicates the data from the FAMOUS area near 36° 50′ N on the MAR (Arcyana, 1977). (▲) indicates data from 45°N on the MAR (Aumento, 1968; Cann, 1970). (●) indicates data from Mid-Indian Oceanic Ridge samples near 12-13°S (Engel and Fisher, 1975). (○) are samples from the Gulf of Aden (Cann, 1970). (C) are samples from the Carlsberg Ridge (Cann, 1969, 1970). (×) are the rocks from the Walvis Ridge (Hekinian, 1972; Hekinian and Thompson, 1976). (N) are average analyses from the Ninety East Ridge (Thompson et al., 1978). (□) indicates data from the Cocos and the Carnegie Ridge samples (Engel and Chase, 1965; Yeats et al., 1973). The field encloses (X), (N), and (□) (aseismic ridge) samples.*

Detrick, R. S. and Lynn, W. S., 1975. The origin of high-amplitude magnetic anomalies at the intersection of the Juan de Fuca Ridge and Blanco fracture zone. *Earth Planet. Sci. Letters,* v. 26, p. 105–113.

Donaldson, D. H., Brown, R. W., and Reid, A. M., 1976. Petrology and chemistry of basalts from the Nazca Plate: Part I, Petrography and mineral chemistry. *In* Yeats, R. S., Hart, S. R., et al., *Initial Reports of the Deep Sea Drilling Project,* v. 34: Washington (U. S. Government Printing Office), p. 227–238.

Engel, C. G. and Chase, T. E., 1965. Composition of basalts dredged from seamounts off the west coast of central America. *U. S. Geol. Surv. Prof. Paper,* v. 525 C, p. 161–163.

Engel, C. G. and Engel, A. E. J., 1961. Composition of basalt cored in Mohole project. *Amer. Assoc. Petroleum Geologists Bull.,* v. 45, (11), p. 1799.

_____, 1963. Basalts dredged from the northeastern Pacific Ocean. *Science,* v. 140, p. 1321–1324.

_____, 1964. Composition of basalts from the Mid-Atlantic Ridge. *Ibid.,* v. 144, p. 1330–1333.

Engel, C. G. and Fisher, R. L., 1975. Granitic to ultramafic rock complexes of the Indian Ocean Ridge System, Western Indian Ocean. *Geol. Soc. Am. Bull.,* v. 86, p. 1553–1578.

Hart, S. R., 1976. LIL-element geochemistry, Leg 34 basalts. *In* Yeats, R. S., Hart, S. R., et al., *Initial Reports of the Deep Sea Drilling Project,* v. 34: Washington (U. S. Government Printing Office), p. 283–288.

Hekinian, R., 1971. Chemical and mineralogical differences between abyssal hill basalts and ridge tholeiites in the eastern Pacific Ocean. *Mar. Geol.,* v. 11, p. 77–91.

Hekinian, R. and Aumento, F., 1973. Rocks from the Gibbs Fracture Zone and the Minia Seamount near 53°N in the Atlantic ocean. *Mar. Geol.,* v. 14, p. 47–72.

Hekinian, R., Moore, J. G., and Bryan, W. B., 1976. Volcanic rocks and processes of the Mid-Atlantic Ridge Rift valley near 36° 49′ N. *Ibid.,* v. 58, p. 83–110.

Hekinian, R. and Thompson, G., 1976. Comparative geochemistry of volcanics from rift valleys transform faults and aseismic ridges. *Contrib. Mineral. Petrol.,* v. 57, p. 145–162.

Kay, R., Hubbard, N. J., and Gast, P., 1970. Chemical characteristics and origin of oceanic ridge volcanic rocks. *J. Geophys. Res.,* v. 75 (8), p. 1581–1613.

Kempe, D. R. C., 1976. Petrological studies on DSDP Leg 34 basalts: Nazca Plate, eastern Pacific Ocean. *In* Yeats, R. W., Hart, S. R., et al., *Initial Reports of the Deep Sea Drilling Project,* v. 34: Washington (U. S. Government Printing Office), p. 189–213.

Luyendyk, B. P. and Engel, C. G., 1969. Petrological magnetic and chemical properties of basalts dredged from abyssal hill in the north-east Pacific. *Nature,* v. 223, p. 1049–1050.

Mazzullo, L. J., 1976. Petrography and phase chemistry of basalts from DSDP Leg 34: Nazca Plate. *In* Yeats, R. W., Hart, S. R., et al., *Initial Reports of the Deep Sea Drilling Project,* v. 34: Washington (U. S. Government Printing Office), p. 245–261.

Melson, W. G., Buerly, G. R., Nelen, J. A., O'Hearn, T., Wright, T. L., and Vallier, T., 1977. A catalog of the major element chemistry of abyssal volcanic glass. *In* Mason, B. (Ed.), Mineral Sciences Investigation, 1974-1975, *Smithsonian Contrib. Earth Sci.,* v. 19, p. 31–60.

Minster, J. B., Jordan, T. H., Molnar, P., and Haines, E., 1977. Numerical modelling of instantaneous plate tectonics. *Geophys J. Roy. Astron. Soc.,* v. 36, p. 541–576.

Miyashiro, A., Shido, F., and Ewing, M., 1969. Diversity and origin of abyssal tholeiite from the Mid-Atlantic Ridge near 24° and 30°N latitude. *Contrib. Mineral Petrol.,* v. 23, p. 38–52.

Moore, J. G., Normark, W. R., Hess, G. R., and Meyer, C. E., 1977. Petrology of basalt from the East Pacific Rise near 21° North latitude. *J. Res. U. S. Geol. Survey,* v. 5 (6), p. 753–759.

Muir, J. D., Tilley, C. E., and Scoon, J. H., 1964. Basalts from the northern part of the Rift zone of the Mid-Atlantic Ridge. *J. Petrol.,* v. 5(3), p. 409–434.

Osborn, E. F. and Tait, D. B., 1952. The system diopside–forsterite–anorthite. *Amer. J. Sci.,* in Bowen volume, p. 413–433.

Pearce, J. A. and Cann, J. R., 1971. Ophiolite origin investigated by discriminant analysis using Ti, Zr and Y. *Earth Planet. Sci. Lett.,* v. 12 (3), p. 339–349.

Pitman, W. C. III, Larson, R. L., and Herron, E. M., 1974. The age of the ocean basins. *Geol. Soc. Am. Charts.*

Poldervaart, A. and Green, J., 1965. Chemical analyses of submarine basalts. *Am. Mineralogist,* v. 50, p. 1723.

Poldervaart, A. and Parker, A. B., 1964. The crystallization index as a parameter of igneous differentiation in binary variation diagram. *Amer. J. Sci.* v. 262, p. 281–289.

Rhodes, J. M., Blanchard, D. P., Rodgers, K. V., Jacobs, J. W., and Brannon, J. C., 1976. Petrology and chemistry of basalts from the Nazca Plate: Part 2, Major and trace element chemistry. *In* Yeats, R. S., Hart, S. R., et al., *Initial Reports of the Deep Sea Drilling Project,* v. 34: Washington (U. S. Government Printing Office), p. 239–244.

Ridley, W. I. and Ajdukiewicz, J., 1976. Preliminary petrology of Leg 34 basalts from the Nazca Plate in DSDP. *In* Yeats, R. S., Hart, S. R., et al., *Initial Reports of the Deep Sea Drilling Project,* v. 34: Washington (U. S. Government Printing Office), p. 277–282.

Scheidegger, K. F., 1973. Temperature and composition of magmas ascending along mid-ocean ridges. *J. Geophys. Res.,* v. 78 (17), p. 3340–3355.

Shido, F., Miyashiro, A., and Ewing, M., 1971. Crystallization of abyssal tholeiites. *Contrib. Mineral Petrol.,* v. 31, p. 251–266.

Thompson, G., Bryan, W. B., Frey, F. A., Dickey J. S., Jr., 1978. Basalts and related rocks from deep-sea drilling sites in the central and eastern Indian Ocean. *Mar. Geol.,* v. 26, p. 119–138.

Thompson, G., Bryan, W. B., Frey, F. A., Dickey, J. S., Jr., and Suen, C. J., 1976. Petrology and geochemistry of basalts from DSDP Leg 34, Nazca Plate. *In* Yeats, R. S., Hart, S. R., et al., *Initial Reports of the Deep Sea Drilling Project,* v. 34: Washington (U. S. Government Printing Office), p. 215–226.

Yeats, R.S., Forbes, W. C., Heath, R. G., and Scheidegger, K. F., 1973. Petrology and geochemistry of DSDP Leg 16 basalts, eastern equatorial Pacific. *In* van Andel, T. H., Heath, G. R., et al., *Initial Reports of the Deep Sea Drilling Project,* v. 16: Washington (U. S. Government Printing Office), p. 617–640.